CORE
Metadata, citation and similar papers at core.ac.uk
Provided by NASA Technical Reports Server

X-661-74-11
PREPRINT

NASA TM X- 70578

A NEW MEASUREMENT OF THE HER X-1 X-RAY PULSE PROFILE

S. S. HOLT
E. A. BOLDT
R. E. ROTHSCHILD
P. J. SERLEMITSOS

FEB 1974
RECEIVED
NASA STI FACILITY
INPUT BRANCH

JANUARY 1974

(NASA-TM-X-70578) A NEW MEASUREMENT OF THE HER X-1 X-RAY PULSE PROFILE (NASA) 11 p HC $3.25 CSCL 03A
N75-12863
Unclas
G3/89 04255

GSFC
GODDARD SPACE FLIGHT CENTER
GREENBELT, MARYLAND

A NEW MEASUREMENT OF THE HER X-1 X-RAY PULSE PROFILE

S. S. Holt, E. A. Boldt, R. E. Rothschild*, and P. J. Serlemitsos
Laboratory for High Energy Astrophysics
NASA/Goddard Space Flight Center
Greenbelt, Maryland 20771

ABSTRACT

We have measured a triple-peaked 1.24 sec. pulse profile in a 1-minute rocket borne exposure to Her X-1, in contrast to the double-peaked profiles expected from models which maximize the X-ray emission at the magnetic equator of an accreting neutron star. The profile exhibits statistically significant energy dependence, with the emission $\geqslant$ 12 keV having narrower peaks which lag (by approximately 5% of the pulse period) the corresponding peaks at lower energies. Approximately one-third of the total emission from the source is non-pulsed.

Subject headings: collapsed stars -- pulsars -- X-ray sources -- binaries

Her X-1 was observed in a rocket-borne experiment launched from White Sands, New Mexico at 0340 UT on 4 October 1973. Two coaligned proportional counters with total net area 1360 cm^2 viewed the source for approximately 58 seconds. One of the counters was filled with 1.1 atm 90% argon-10% methane, and possessed a mechanical collimator which limited its field of view to 2°x8° FWHM; the other was filled with 1.1 atm 90% xenon-10% methane, and possessed a 3° FWHM circular collimator. During the entire exposure, the pointing was held to ± 10 sec. by the rocket guidance system, so no temporal variations in

*NAS-NASA Postdoctoral Resident Research Associate

the counting rate may be attributable to jitter in the rocket attitude. Using the 1.700165d and 35.7d periods given by Giacconi et al. (1973) and the reference epochs of Tananbaum et al. (1972), the present exposure corresponds to a phase of 0.6 $\pm$0.03 in the 1.7d eclipse period (referenced to minimum center), and is close to the center of the ~ 1/3 duration on-state of the 35.7d variation.

The data were searched for periodic components using fast-Fourier and fast-fold algorithms, as described in Holt et al. (1973). At 99% confidence, no periodic components down to ~ 1 msec. were detected at a level exceeding a pulsed fraction of ~ 10% which were not directly attributable to the 1.24 sec. variation. The latter periodicity was detected at an apparent period of 1.2372 $\pm$.001 sec., with the uncertainty being a function solely of the small number of pulse periods in the exposure. The ultimate temporal resolution of the telemetry record, 320 μsec, could not be usefully applied to variations on a time scale as large as 1.24 sec.

In Figure 1, data from precisely 44 periods are folded modulo the apparent period of 1.2372 sec. All seven traces are without background subtracted, and the appropriate background level is noted in each case. The uppermost trace is the total count accumulated in the entire record, with a temporal resolution of 12.4 msec. (i.e. 1% of the pulse period). The next two traces are the same data from only the first and last quarters of the exposure, respectively. Also plotted are the data in four different energy bins for the entire 44 periods: 1.5-3 keV, 3-6 keV, 6-12 keV and 12-35 keV. Of these four, only the two intermediate energy windows have relatively flat responses over their entire range. Because counter characteristics bias the response functions of the other two energy ranges, we have labelled these two traces $\leq$ 3 keV and $\geq$ 12 keV to reflect the higher efficiency at the noted window extremes.

Chi-square tests verify the visual indication from the three uppermost traces of Figure 1 that there is no apparent systematic variation in the overall pulse profile during the ~ 1 minute of data accumulation. Relative stability of the pulse profile on this time scale has been previously noted by Doxsey et al. (1973), and by Giacconi et al. (1973). Similarly, the general pulse features are grossly consistent with the light curves published by these two groups, as can be observed from Figure 2. The present data (trace D) contain a broad (~ 2/5 of the pulse period) double-peaked emission feature, and an "interpulse" ~ 180° out of phase with the primary emission. Doxsey et al. have reported a similar double-peaked primary (with phase separation ~ 90°, as in the present data), but no distinguishable interpulse (trace C). Giacconi et al. (1973) have reported two ~ one-minute exposures separated by about 1 1/2 hours. The earlier of these (trace B) is qualitatively similar to the Doxsey et al. measurement, except that the phase separation of the pulses is only ~ 60°. The other (trace A) has a single-peaked main emission feature, with an interpulse ~ 180° out of phase which is lacking in the earlier exposure.

Owing to the extended energy response and low non-Her X-1 background of the present measurement, the data may be investigated in greater detail than previously possible with respect to the energy dependence of the pulse profile. The four lower traces of Figure 1 give the general indications that emission at higher energies is both better defined (i.e. narrower pulses) and lags in phase with respect to emission at lower energies. This latter effect is demonstrated in Figure 2, where the $\leqslant$ 3 keV, 6–12 keV and $\geqslant$ 12 keV profiles are compared with that of 3–6 keV (which of the four ranges, should most closely replicate the UHURU detector response). The observed 3–6 keV pulse profile is plotted for reference (with background subtracted) in units of the fraction of the total emission in each of the 25 bins into which the pulse profile has been divided (i.e. the total area of the exhibited pulse profile is unity). The other three profiles are plotted as decrements with respect to the 3–6 keV profile, in units of the number of Poisson sigmas which characterize each point. If, in the i'th light curve bin, the fraction of the total Her X-1 emission in the 3–6 keV range is g_i and in another energy range is f_i (with the errors after background subtraction being δg_i and δf_i, respectively), what is plotted in Figure 3 is:

$$S_i = \frac{g_i - f_i}{\sqrt{\delta^2 g_i + \delta^2 f_i}} \quad . \tag{1}$$

All deviations in excess of 1σ have been shaded to aid the eye in determining the general trends.

The $\geqslant$ 12 keV trace clearly exhibits deficiencies with respect to the 3–6 keV profile at the leading edge of all three peaks in the profile. In addition, there is a definite excess at the trailing edge of the first peak in the primary component. With respect to the peak positions alone, there appears to be a phase lag of ~ 5% of the pulse period in the $\geqslant$ 12 keV emission relative to that in the 3–6 keV band.

The 6–12 keV trace exhibits much better agreement with 3–6 keV than does ⩾ 12 keV, but the largest deviations are consistent with the largest deviations in the higher energy comparison: excess emission at the trailing edge of the first primary peak, and an emission deficiency at the leading edge of the second primary peak.

The ⩽ 3 keV trace exhibits two effects which may each be separately interpretable. The largest decrement is at the trailing edge of the second primary peak, which is consistent with the systematic energy dependence discussed above. The decrement at the leading edge of the first primary component peak is not: the ⩽ 3 keV rise time to this peak is more sluggish than in the range 3–12 keV. Doxsey et al. (1973) and Giacconi et al. (1973) have pointed out that the primary component peaks in their measurements have a rise time larger than the fall time (particularly for the second primary peak). In the present case, the second parimary peak is not well-enough defined to determine its rise time, but the first primary peak appears to have a rise time which exceeds its fall time only for the extreme energy ranges ⩽ 3 keV and ⩾ 12 keV.

All other fluctuations in Figure 3 are consistent with statistical variations. In particular, the excess in all three comparisons at the trailing edge of the interpulse may arise from a statistical fluctuation in the 3–6 keV profile and, since this (rather than a smoothed profile) was subtracted to produce the three comparison traces, a modest excess for all of them in this bin is not surprising.

There appears to be a substantial "non-pulsed" component to the source emission during the present exposure. If we assume that the lowest bin in the 3–6 keV trace of Figure 3 is non-pulsed, the total fraction of the light curve which is included in this non-pulsed component is 0.36 $\pm$0.05. There is no statistically significant energy dependence (as defined in Eq. 1) to this baseline intensity.

We measure an overall energy spectrum (the details of which will be presented elsewhere) consistent with previously reported Her X-1 high-state spectra. The relatively flat ($\sim E^{-1}$) continuum with a pronounced deficiency above ~ 20 keV (as reported by Ulmer et al., 1973) may be reconciled with accretion models in which the X-ray emission is produced in a relatively small volume above the stellar poles. The observed continuum is then the integrated emission from the source "layers" transported through the gas in the source neighborhood up to the ~ 20 keV energy corresponding to free-fall to the base of the source region. In Davidson's (1973) discussion of such a model, he points out that since a layer deeper in the source is predominantly responsible for higher energy emission, it might be expected that such emission will have narrower peaks in the pulse profile. The phase lag we observe at higher energies may be a manifestation of the same effect. Similarly, the non-zero baseline and the sluggish rise of the main peak at lower energies may be ultimately attributable to the detailed photon transport from the emission region.

While there remain many unresolved issues for the Hz Her-Her X-1 system as a whole, with regard to <u>only</u> the pulse profile there would appear to remain two problems for which the type of model discussed above has no obvious qualitative explanation: the observation of more than two peaks in the present measurement, and the variation in pulse profile on time scales of hours or less.

REFERENCES

Davidson, K., 1973, Nature (Phys. Sci.) 246, 1.

Doxsey, R., Bradt, H. V., Levine, A., Murthy, G. T., Rappaport, S., Spada, G., 1973, Ap. J. (Letters), 182, L25.

Giacconi, R., Gursky, H., Kellogg, E., Levinson, R., Schreier, E., and Tananbaum, H., 1973, Ap. J. 184, 227.

Holt, S. S., Boldt, E. A., Serlemitsos, P. J., and Brisken, A. F., 1973, Ap. J. (Letters), 180, L69.

Tananbaum, H., Gursky, H., Kellogg, E. M., Levinson, R., Schreier, E., and Giacconi, R., 1972, Ap. J. (Letters), 174, L143.

Ulmer, M. P., Baity, W. A., Wheaton, W. A., and Peterson, L. E., 1973, Ap. J. (Letters), 181, L33.

FIGURE CAPTIONS

Fig. 1 The present data folded modulo 1.2372 sec. The three uppermost traces are all photons detected in the energy range 1.5-35 keV for all 44 pulse periods, the first 11 periods, and the last 11 periods, respectively. The remaining four traces are data from all 44 pulse periods in the indicated energy ranges. The non-Her X-1 background for each trace is indicated with a B.

Fig. 2 1.24 sec. light curves from three different experiments in comparable energy ranges. Traces A and B are taken from Giacconi et al. (1973), and are each ~ one-minute UHURU exposures separate by ~ 1 1/2 hours. Trace C is taken from Doxsey et al. (1973), and Trace D is the present data (the same as the heavily shaded trace of Figure 3). The phases of Traces C and D have been chosen arbitrarily with respect to those of A and B.

Fig. 3 Background-subtracted 1.2372 sec. light curves in the four energy ranges considered, as described in the text. The heavy-shaded trace is the 3-6 keV profile normalized so that its total area is unity. The remaining traces are plotted as the difference between the similarly normalized profiles in the indicated energy ranges and the 3-6 keV profile, in units of Poisson sigmas. All variations in excess of 1σ are shaded to aid the eye in the determination of general trends.

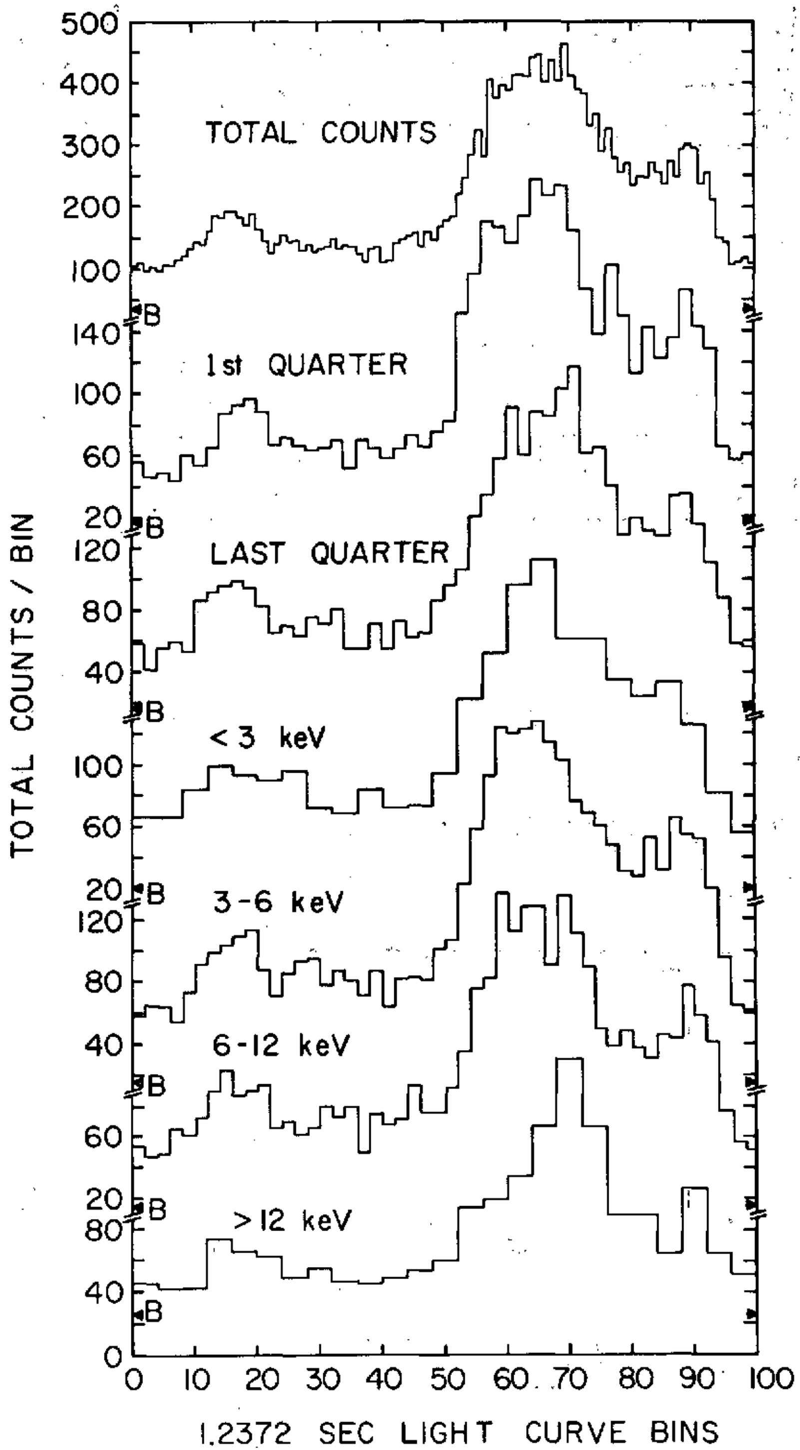
TOTAL COUNTS
1st QUARTER
LAST QUARTER
< 3 keV
3-6 keV
6-12 keV
> 12 keV
TOTAL COUNTS / BIN
1.2372 SEC LIGHT CURVE BINS

Figure 1

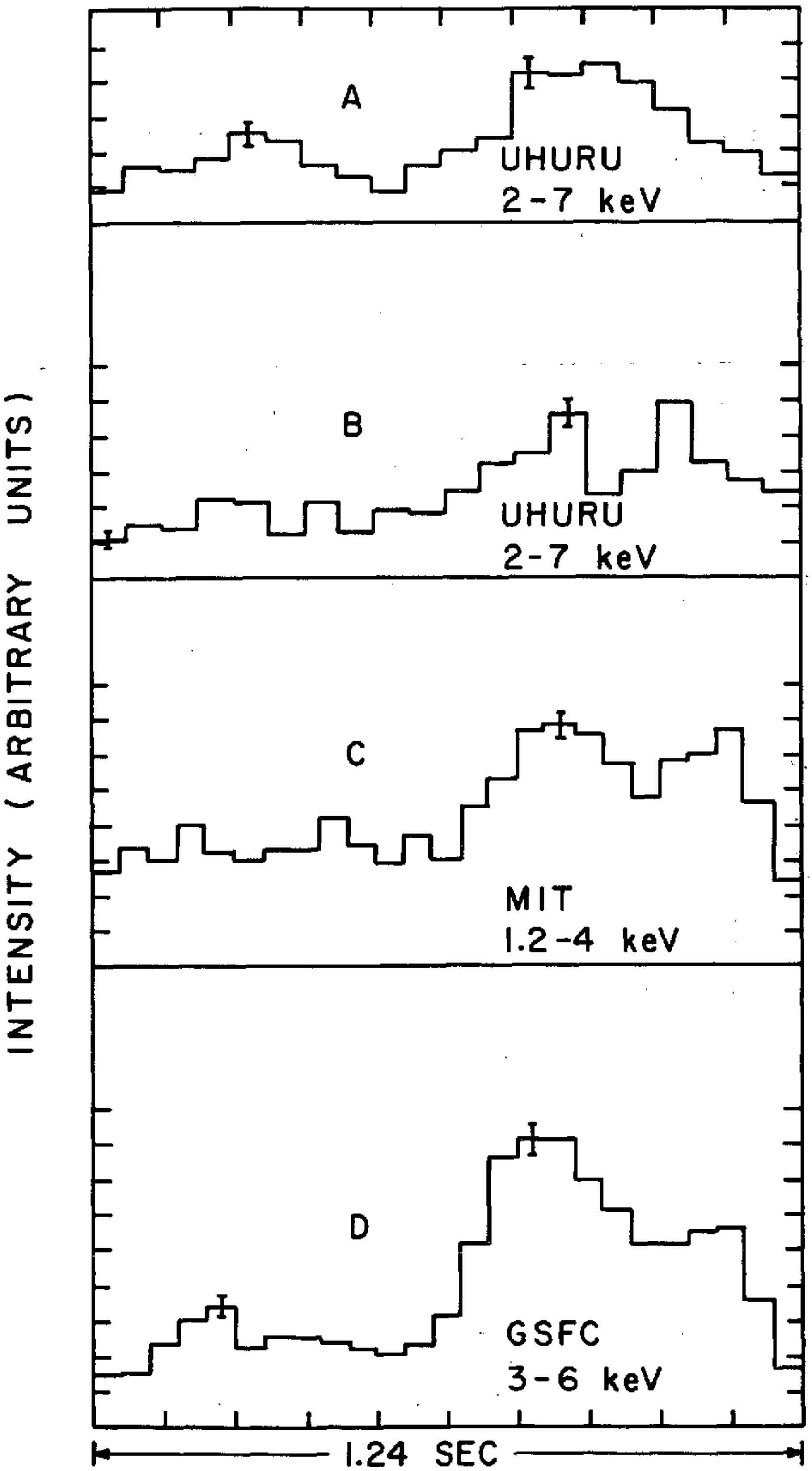

INTENSITY (ARBITRARY UNITS)
A
UHURU
2-7 keV
B
UHURU
2-7 keV
C
MIT
1.2-4 keV
D
GSFC
3-6 keV
1.24 SEC

Figure 2

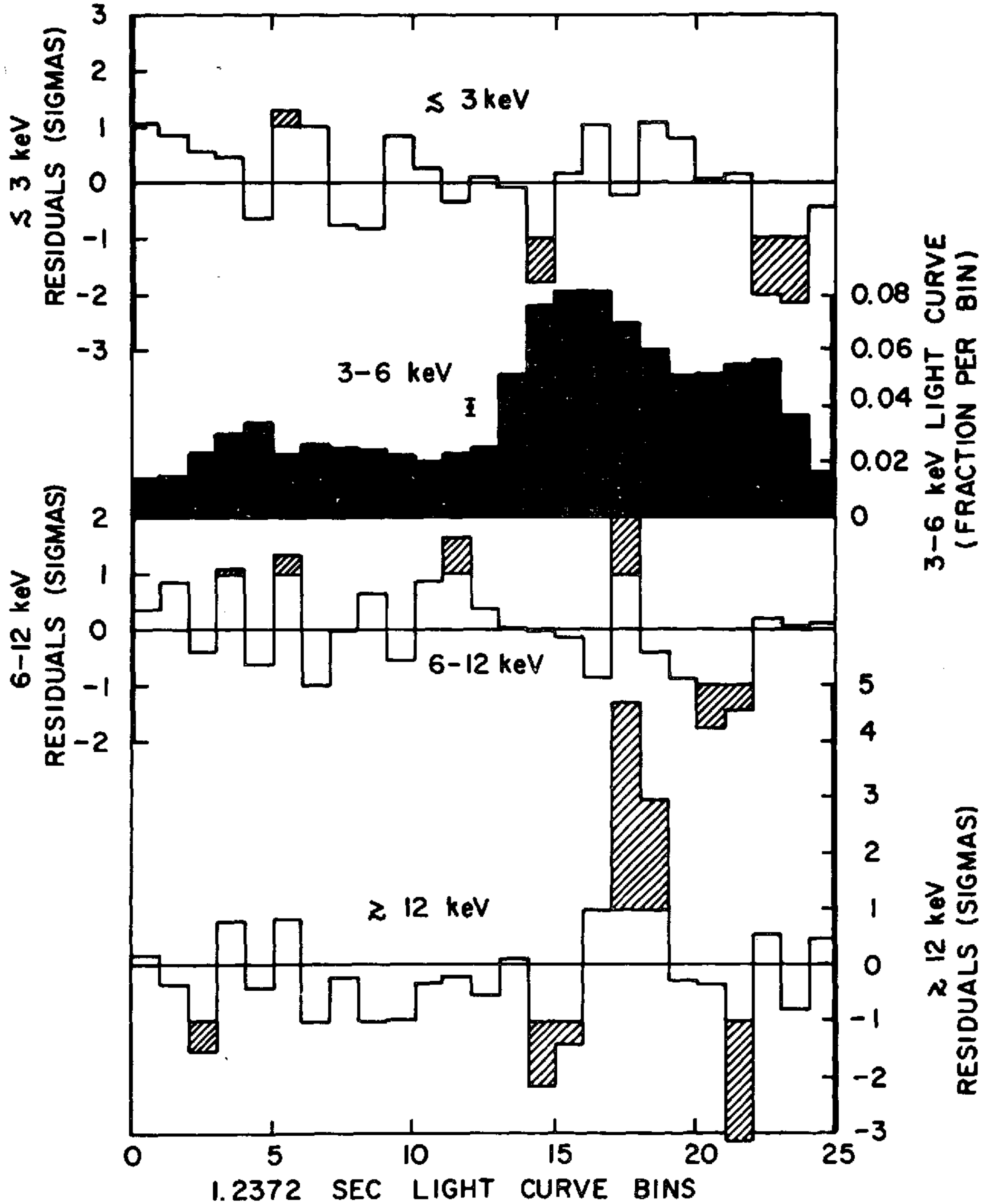
≲ 3 keV
RESIDUALS (SIGMAS)
≲ 3 keV
3-6 keV
3-6 keV LIGHT CURVE
(FRACTION PER BIN)
0.08
0.06
0.04
0.02
6-12 keV
RESIDUALS (SIGMAS)
6-12 keV
≳ 12 keV
≳ 12 keV
RESIDUALS (SIGMAS)
1.2372 SEC LIGHT CURVE BINS
0
5
10
15
20
25

Figure 3